Available online at www.sciencedirect.com

ScienceDirect

Procedia Materials Science 3 (2014) 1848 – 1853

Procedia Materials Science

www.elsevier.com/locate/procedia

20th European Conference on Fracture (ECF20)

Fracture energy of graphite from microstructure-informed lattice model

Craig N Morrison*, Mingzhong Zhang, Andrey P Jivkov

Mechanics and Physics of Solids Research Team, School of Mechanical, Aerospace and Civil Engineering, The University of Manchester, Manchester, M13 9PL, UK

Abstract

Graphite remains a key structural material in the nuclear industry, the integrity assessment of which in demanding reactor environments is critical for safe operation of plant. Fracture of graphite is preceded by growth and coalescence of distributed micro-cracks within a process zone, classifying it as a quasi-brittle material alongside cement-based and ceramic materials. The evolution of a micro-crack population to failure is well represented by discrete lattice models, e.g. (Wang and Mora 2008). Here, a recently developed 3D lattice (Jivkov and Yates 2012), with elastic spring elements and brittle-damage behaviour is used to generate microstructure representative models of two graphite grades at a representative meso length scale. Micro-cracks are represented by spring failures and the macroscopic damage results from their collective behaviour. Presented results capture a transition from graceful, plastic-like failure at lower porosities, with energy dissipation via micro-cracking, to glass-like behaviour with negligible energy dissipation at higher porosities. The results are in good agreement with experimental data. Thus, the proposed methodology can calculate fracture energy from the stress-strain curve, or formulate cohesive and damage evolution laws for continuum models, based exclusively on microstructural features.

Selection and peer-review under responsibility of the Norwegian University of Science and Technology (NTNU), Department of Structural Engineering

Keywords: Nuclear graphite; Porosity; Meso-scale model; Quasi-brittle behaviour; Damage evolution

* Corresponding author.
E-mail address: craig.morrison@manchester.ac.uk

Selection and peer-review under responsibility of the Norwegian University of Science and Technology (NTNU), Department of Structural Engineering
doi:10.1016/j.mspro.2014.06.298

1. Introduction

Nuclear-grade graphite has been used as both a fast neutron moderator and structural material in over 100 reactors worldwide. The ability to fulfill both purposes gives it a distinct advantage over water-based reactors and has lead to its inclusion in the design of the Generation IV Very High Temperature Reactor. Consequently both future reactor core designs and life extensions of existing plants require a suitable means of predicting the structural integrity of graphite in the demanding environment and complex loading states found in a reactor core.

Graphite has a feature-rich microstructure consisting of multiple phases, the size and structure of which are dependent upon the raw materials and manufacturing process used. This has allowed for the development of a broad range of graphite grades, with properties tailored to a specific purpose. The microstructure consists of filler particles, derived from petroleum or pitch cokes distributed within a matrix of graphitized binder material; usually coal-tar pitch. Distributed throughout both of these phases are 3 main populations of porosity formed at different stages of the manufacturing process; gas evolution cracks, calcinations cracks and Mrozowski cracks (Bradford and Steer 2008; Joyce et al. 2008), the length scale of which ranges from nm to mm scale depending on the grade in question.

Current preferred modeling procedures used to investigate component scale integrity are based on a classical continuum, such as the finite element method. These inherently fail to model the effect of microstructure on macroscopic behavior, assuming all points in an element behave homogeneously. This is problematic when modeling graphite components where failure has been shown to be dependent on its discrete multiphase microstructure (Mostafavi and Marrow 2012), primarily the result of micro-crack coalescence into a critically sized flaw. Such a response suggests graphite falls into the class of quasi-brittle materials alongside rock, concrete and ceramics. Upon loading quasi-brittle materials typically exhibit a reduction of stiffness prior to failure, similar to plasticity. Moreover, a residual load carrying capacity beyond the peak load is demonstrated (Hodgkins et al. 2010).

Attempts have been made at developing continuum-based approaches which account implicitly for microstructural affects, notably in the fracture process zone (FPZ) ahead of an existing crack. One approach of note, easily implemented in the finite element method is cohesive zone modeling (Borst 2002; Elices et al. 2002). This method represents the local softening found in quasi-brittle materials ahead of a crack in the properties of cohesive elements. However problems arise from the pre-definition of a crack path and the phenomenological calibration and curve fitting of parameters required from observed macroscopic behavior for different loading cases.

Such failings of continuum approaches have led to the development of a number of local fracture models for quasi-brittle materials. These ‘meso-scale’ models aim to capture the dependence of macro- or component scale failure on microstructural features by representing the corresponding failure mechanisms at the feature length scale in a physically realistic manner (Lemaitre 1986). However, most current local approaches are again phenomenological (Borst 2002) and as such inherently ignore the actual failure mechanisms observed at the microscale of quasi-brittle materials (Bažant and Pang 2007). Microstructure-informed models, such as the one offered in this work, have the potential to assist in deriving mechanistic constitutive laws suitable for use in the aforementioned continuum approaches such as cohesive zone modeling.

Lattice models, such as the model described in this paper, are a category of local discrete models, where discrete elements, including springs (Pazdniakou and Adler 2012) and beams (Schlangen and Garboczi 1997) are used as connections between nodes to form a parallel network. The response and failure of elements can incorporate actual mechanisms at the length scale of microstructure features, allowing a physically realistic macro-mechanical response. Global failure is the result of cumulative micro-failures into a macro-sized flaw, with load redistribution occurring upon failure of single bonds. Previous lattice models for graphite (Nemeth and Bratton 2010) and concrete (Schlangen and Garboczi 1997) have either been 2D models, questionable in their ability to simulate the intrinsically 3D phenomenon of micro-crack damage evolution, or limited in their ability to reproduce a full range of Poisson’s ratio for elastic materials (Wang and Mora 2008).

This work extends the site-bond 3D lattice model developed by Jivkov and Yates (Jivkov and Yates 2012) with application to nuclear graphite using bundles of springs as discrete bonds connecting sites at the centre of unit cells. Previous construction methodology accounting for experimentally measured particle and pore size distributions is improved (Morrison et al. 2014b; Morrison et al. 2014a) and used to investigate the effects of increasing porosity on tensile strength and damage evolution with a view to understanding graphite’s response to radiation damage.

2. Theory and Model

The theory behind the site-bond model is briefly presented here. Details are given in another contribution to this volume (Jivkov et al. 2014) and in previous works (Jivkov and Yates 2012; Morrison et al. 2014a; Morrison et al. 2014b). The model consists of a regular tessellation of truncated octahedral cells – the regular shape considered the closest representation of a generic microstructure (Kumar et al. 1992). The truncated octahedron has six square faces, normal to the principle axes, and eight hexagonal faces, normal to the octahedral axes. Sites at cell centers are connected to neighboring sites by bonds, with bond lengths varying for principal and octahedral directions.

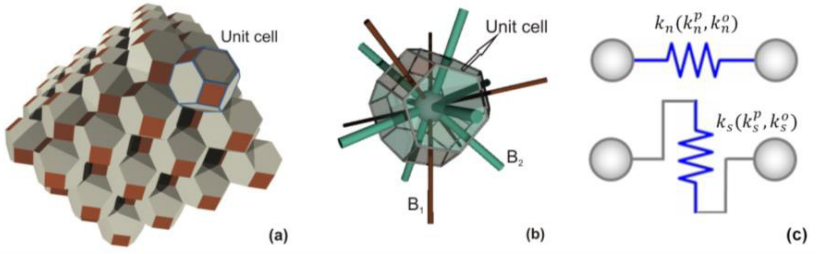

Fig. 1. Cellular lattice: (a) site-bond assembly; (b) unit cell with bonds; (c) normal and shear springs.

In this work each bond is represented as a bundle of elastic-brittle normal and shear spring. The need for further angular springs to represent all degrees of freedom between sites is a subject of ongoing work. Spring constants, given in Eq.1, are calibrated by equating the strain energy in a single discrete cell to the energy in the equivalent continuum (Zhang et al. 2013).

$$k_n^p = \frac{EL}{4(1+\nu)(1-2\nu)}; \quad k_s^p = 0; \quad k_n^o = \frac{(1+2\nu)EL}{4(1+\nu)(1-2\nu)}; \quad k_s^o = \frac{(1-4\nu)EL}{4(1+\nu)(1-2\nu)} \tag{1}$$

where E and ν are Young's modulus and Poisson's ratio of the material respectively, k_n^p and k_s^p represent the stiffness of normal and shear springs in principal directions and k_n^o and k_s^o represent the stiffness of normal and shear springs in octahedral directions. L is the cell size, i.e. distance between sites in the principal directions.

3. Distribution of Material Features

Experimentally measured particle and pore size distributions, reproduced from (Kane et al. 2011) for two graphite grades, IG110 and PGX, were used to microstructurally inform corresponding site-bond models at increasing pore volume fractions (porosity) in order to simulate the effect of radiation damage. A meso-length scale was naturally introduced by randomly assigning particles to sites of a lattice of specified size, in this case 15 x 15 x 15 cells. The cell size was calculated by equating the specified particle volume fraction of each grade with the known volume of the distributed pores and lattice size (Morrison et al. 2014b). A consistent cell size was used for each grade of graphite to allow direct comparison between cases of varying porosity. Pores were randomly distributed to faces between cells over a succession of passes, with multiple pores allocated to each face to ensure the desired porosity was reached. Each pore is assumed spherical and bisected by cell faces such that the pore cross-sectional area on each face is maximum. In a previous work (Morrison et al. 2014b) springs without a pore present fail at a prescribed energy, namely the product of the cell face area through which the bond passes and the graphite energy of separation (Abrahamson 1973). This produced tensile strengths of half the experimentally measured values. Here, each spring was allowed double the peak force of previous works, corresponding to a factor of four increase in failure energy when springs constants are maintained. The presence of pores on a cell face is incorporated into the corresponding spring failure criteria. Failure energy decreases from the pore-free value according to the ratio of the face area which is pore-free and the total face area. The material properties used for calibration of each grade and key statistical parameters are given in Table 1.

Table 1. Material properties and microstructure data for IG110 and PGX graphite.

Grade	IG110	PGX	Reference
Elastic modulus E (MPa)	9800	8300	(Products n.d.), (Kaji et al. 2001)
Poisson's ratio ν	0.14	0.11	(Products n.d.), (Kaji et al. 2001)
Mean particle diameter (μm)	27	92	(Kane et al. 2011)
Mean pore area (μm^2)	98	197.9	(Kane et al. 2011)
Particle volume fraction	20%	20%	(Kane et al. 2011)
Porosity in virgin state	14.73%	21.49%	(Kane et al. 2011)

4. Results and Discussion

Fig. 2 shows the simulated stress-strain curves for specimens with different porosities. At lower porosity values both grades exhibit a typically 'graceful' quasi-brittle response, with pre-peak softening similar to plasticity. As porosity increases this shifts to a more brittle response with minimal energy dissipation corresponding to avalanche-failure of multiple bonds. Simulations at each porosity were repeated with different spatial distributions of pores to check the validity of a lattice of 15 cell length as a representative volume element (RVE). The stress strain response remained consistent for both grades at every porosity value, although there was variation in the tensile strength of the IG110 grade at a given porosity. This suggests that the model size for IG110 is not an RVE with respect to damage evolution. The failure to capture potential post-peak softening in the stress-strain curves is a subject of ongoing work, including the consideration of more representative failure criteria derived from lower scale simulations. Inclusion of a softening tail to the response will allow derivation of mechanistic constitutive laws for continuum damage modelling of fracture.

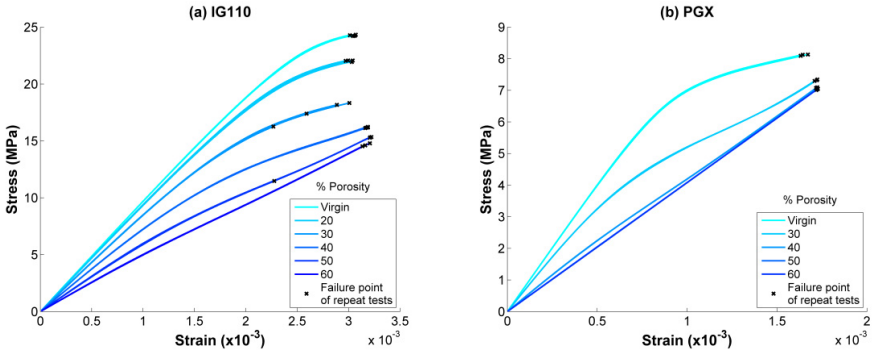

Fig. 2. Stress-strain response to failure for: (a) IG110; (b) PGX at varying levels of porosity.

The introduction of an improved failure criterion has resulted in a good match between obtained tensile strength values at the virgin state and experimental data (Ishihara et al. 2004). As porosity θ is increased the change in tensile strength has been shown to exponentially decay approaching zero (Berre et al. 2008; Ishihara et al. 2004) according to the Knudsen relationship (Knudsen 1959), Eqn. 2. The results obtained from our model, Fig. 3, demonstrate a similar exponential decay, however the end value is non-zero such that the approximation in Eqn. 3. is followed, where m equals 5 and 9 for IG110 and PGX respectively. The reason for this is that the model possesses a resistance to instantaneous failure due to a number of bonds without pores even at high porosities. Even if the failure is of avalanche type, the system requires external work to overcome the failure energies assigned to these bonds. By increasing the porosity an improved estimate can be obtained.

$$\sigma_f = \sigma_{f0} e^{-m\theta} \tag{2}$$

$$\sigma_f = \sigma_{f0}\left(e^{-m\theta} + \left(1 - e^{-m\theta_0}\right)\right) \tag{3}$$

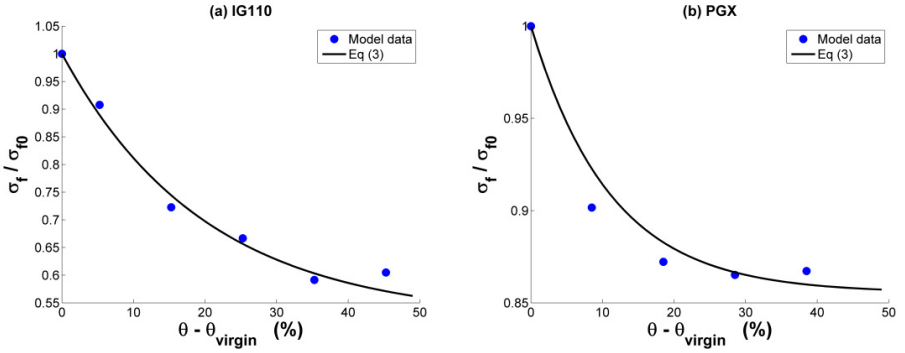

Fig. 3. Relationship between tensile strength and porosity for: (a) IG110; (b) PGX.

Fig. 4 illustrates the evolution of damage for both grades at each value of porosity, where damage is defined at the relative degradation of the corresponding Young's modulus. At low porosity in IG110 the damage evolves at an ever increasing rate until failure. As porosity increases damage evolution again starts at any increasing rate, however prior to failure the evolution rate begins to decrease. As porosity progressively increases this declining rate of increase occurs faster as the material's response becomes more brittle. The response of PGX appears similar with a quicker decline to a brittle response. The results suggest this model can be used to analyse and further understand damage evolution ahead of a macroscopic crack for a material of known microstructure with a possibility to aid in the prediction of FPZ size – a phenomenon not yet fully understood in quasi-brittle materials (Awaji et al. 2006).

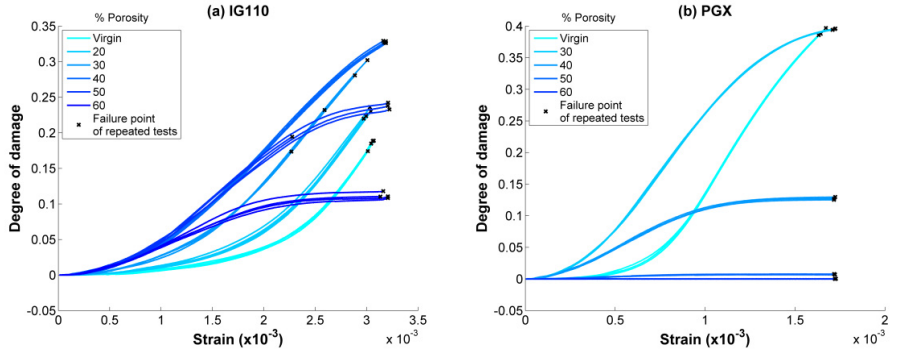

Fig. 4. Damage evolution for: (a) IG110; (b) PGX; at various porosities.

5. Conclusions

This work describes a method of constructing a site-bond model to account for experimentally measured pore and particle size distributions and volume fractions, such that a suitable meso-scale length scale is achieved. We have demonstrated its potential to derive material constitutive behavior emerging from micro-crack growth and coalescence – the prominent microstructural failure mechanism for quasi-brittle materials, such as graphite. Two graphite grades have been investigated, with 'graceful' quasi-brittle found at lower porosities whereby energy is dissipated with distributed micro-failures and hence an increasing rate of damage evolution prior to global failure. Increase of porosity leads to a more brittle response where final failure is sudden with avalanche-like failure of numerous bonds simultaneously. In this case, rate of damage evolution is constantly decreasing. Tensile strength is shown to exponentially decay with increased porosity, although the decay relationship differs from literature data.

The method has potential for use in exploring phenomena which are not currently well understood, e.g. the FPZ size, and deriving constitutive and damage evolution behavior for a microstructure under aging processes for use in continuum methods. Further work includes; additional consideration of angular spring inclusion on receipt of experimental evidence exhibiting graphite's characteristics as a generalized continuum and exploration of the correct surface energy of graphite required for deriving spring failure criteria.

Acknowledgements

Morrison appreciates the support from EPSRC via Nuclear FiRST Doctoral Training Centre. Zhang and Jivkov acknowledge the support from EPSRC via grant EP/J019763/1, "QUBE: Quasi-Brittle fracture: a 3D experimentally-validated approach", and from BNFL for the Research Centre for Radwaste & Decommissioning.

References

Abrahamson, J., 1973. The surface energies of graphite. *Carbon*, 11(4).

Awaji, H., Matsunaga, T., Choi, S.-M., 2006. Relation between Strength, Fracture Toughness, and Critical Frontal Process Zone Size in Ceramics. *Materials Transactions*, 47(6), pp.1532–1539.

Bažant, Z.P., Pang, S., 2007. Activation energy based extreme value statistics and size effect in brittle and quasibrittle fracture. *Journal of the Mechanics and Physics of Solids*, 55(1), pp.91–131.

Berre, C., Fok, S.L., Mummery, P.M., Ali, J., Marsden, B.J., Marrow, T.J., Neighbour, G.B., 2008. Failure analysis of the effects of porosity in thermally oxidised nuclear graphite using finite element modelling. *Journal of Nuclear Materials*, 381(1-2), pp.1–8.

Borst, R. de, 2002. Fracture in quasi-brittle materials: a review of continuum damage-based approaches. *Engineering fracture mechanics*, 69, pp.95–112.

Bradford, M.R., Steer, A.G., 2008. A structurally-based model of irradiated graphite properties. *Journal of Nuclear Materials*, 381(1-2), pp.137–144.

Elices, M., Guinea, G.V., Gómez, J., Planas, J., 2002. The cohesive zone model: advantages, limitations and challenges. *Engineering Fracture Mechanics*, 69(2), pp.137–163.

Hodgkins, A., Marrow, T.J., Wootton, M.R., Moskovic, R., Flewitt, P.E.J., 2010. Fracture behaviour of radiolytically oxidised reactor core graphites: a view. *Materials Science and Technology*, 26(8), pp.899–907.

Ishihara, M., Sumita, J., Shibata, T., Iyoku, T., Oku, T., 2004. Principle design and data of graphite components. *Nuclear Engineering and Design*, 233(1-3), pp.251–260.

Jivkov, A.P., Morrison, C.N., Zhang, M., 2014. Site-bond modelling of structure-failure relations in quasi-brittle media. In *20th European Conference on Fracture, Trondheim, Norway*. p. Paper #689.

Jivkov, A.P., Yates, J.R., 2012. Elastic behaviour of a regular lattice for meso-scale modelling of solids. *International Journal of Solids and Structures*, 49(22), pp.3089–3099.

Joyce, M.R., Marrow, T.J., Mummery, P., Marsden, B.J., 2008. Observation of microstructure deformation and damage in nuclear graphite. *Engineering Fracture Mechanics*, 75(12), pp.3633–3645.

Kaji, Y., Gu, W., Ishihara, M., Arai, T., Nakamura, H., 2001. Development of structural analysis program for non-linear elasticity by continuum damage mechanics. *Nuclear Engineering and Design*, 206(1), pp.1–12.

Kane, J., Karthik, C., Butt, D.P., Windes, W.E., Ubic, R., 2011. Microstructural characterization and pore structure analysis of nuclear graphite. *Journal of Nuclear Materials*, 415(2), pp.189–197.

Knudsen, F.P., 1959. Dependence of Mechanical Strength of Brittle Polycrystalline Specimens on Porosity and Grain Size. *Journal of the American Ceramic Society*, 42(8), pp.376–387.

Kumar, S., Kurtz, S.K., Banavar, J.R., Sharma, M.G., 1992. Properties of a three-dimensional Poisson-Voronoi tesselation: A Monte Carlo study. *Journal of Statistical Physics*, 67(3-4), pp.523–551.

Lemaitre, J., 1986. Local approach of fracture. *Engineering Fracture Mechanics*, 23, pp.523–537.

Morrison, C.N., Jivkov, A.P., Smith, G., Yates, J.R., 2014a. Lattice-spring modeling of graphite accounting for pore size distribution. *Key Engineering Materials*, 592-593, pp.92–95.

Morrison, C.N., Zhang, M., Jivkov, A.P., Yates, J.R., 2014b. A Discrete Lattice Model of Quasi-brittle Fracture in Porous Graphite. *Materials Performance and Characterisation*, 3(3), p.In press.

Mostafavi, M., Marrow, T.J., 2012. Quantitative in situ study of short crack propagation in polygranular graphite by digital image correlation. *Fatigue & Fracture of Engineering Materials & Structures*, 35(8), pp.695–707.

Nemeth, N.N., Bratton, R.L., 2010. Overview of statistical models of fracture for nonirradiated nuclear-graphite components. *Nuclear Engineering and Design*, 240(1), pp.1–29.

Pazdniakou, A., Adler, P.M., 2012. Lattice Spring Models. *Transport in Porous Media*, 93(2), pp.243–262.

Products, Toyo Tanso Carbon., Special Graphite and Compound Material Products.

Schlangen, E., Garboczi, E., 1997. Fracture simulations of concrete using lattice models: computational aspects. *Engineering Fracture Mechanics*, 57(2), pp.319–332.

Wang, Y., Mora, P., 2008. Macroscopic elastic properties of regular lattices. *Journal of the Mechanics and Physics of Solids*, 56(12), pp.3459–3474.

Zhang, M., Morrison, C.N., Jivkov, A.P., 2013. A meso-scale site-bond model for elasticity: Theory and calibration. *Material Research Innovations*, In press.